Intelligent Bearing Fault Diagnosis Method Based on HNR Envelope and Classification Using Supervised Machine Learning Algorithms

Ilias OUACHTOUK[1] iD, Soumia EL HANI[1] iD, Khalid DAHI[2] iD

[1]Electrical Laboratory Research, Ecole Nationale Superieure des Arts et Metiers, Mohammed V University, Avenue des Nations Unies, Agdal, 10000 Rabat, Morocco
[2]Complex System and Interactions, Ecole Centrale of Casablanca, Ville Verte, Bouskoura, 20000 Casablanca, Morocco

ilias_ouachtouk@um5.ac.ma, s.elhani@um5s.net.ma, khalid.dahi@centrale-casablanca.ma

Abstract. *Research on data-driven bearing fault diagnosis techniques has recently drawn more and more attention due to the availability of massive condition monitoring data. The research work presented in this paper aims to develop an architecture for the detection and diagnosis of bearing faults in the induction machines. The developed data-oriented architecture uses vibration signals collected by sensors placed on the machine, which is based, in the first place, on the extraction of fault indicators based on the harmonics-to-noise ratio envelope. Normalisation is then applied to the extracted indicators to create a well-processed data set. The evolution of these indicators will be studied afterwards according to the type and severity of defects using sequential backward selection technique. Supervised machine learning classification methods are developed to classify the measurements described by the feature vector with respect to the known modes of operation. In the last phase concerning decision making, ten classifiers are tested and applied based on the selected and combined indicators. The developed classification methods allow classifying the observations, with respect to the different modes of bearing condition (outer race, inner race fault or healthy condition). The proposed method is validated on data collected using an experimental bearing test bench. The experimental results indicate that the proposed architecture achieves high accuracy in bearing fault detection under all operational conditions. The results show that, compared to some proposed approaches, our proposed architecture can achieve better performance overall in terms of the number of optimal features and the accuracy of the tests.*

Keywords

Bearing, harmonics-to-noise ratio envelope, induction machines, Supervised Machine Learning, vibration.

1. Introduction

Electric machines cover a wide range of economic activities in almost all industrial sectors, of which the majority are electric motors. According to ADEME (Agence de l'Environnement et de la Mai+ trise de l'Energie) studies in France, these motors account for 70 % of the total electricity consumption in the industrial sector [1]. This shows that it is essential to continuously monitor these machines in order to detect faults and degradations. From this perspective, this study focuses on asynchronous electric motors with squirrel cage rotors. Indeed, electric motors are used as main actuators in more than 90 % of mechanical drives in industries worldwide. The most common mechanical units in industries that are driven by an electric motor are compressors (air or other fluids), pumps and fans [2] and [3].

Bearing faults account for over 51 % of all electric motor defects [4]. The majority of bearings in industrial installations operate under non-ideal conditions and are subject to fatigue, ambient mechanical vibration, overload, misalignment, pollution, corrosion, and inadequate lubrication. These non-ideal conditions

start with minor defects that propagate to the bearing outer ring, inner ring and rolling elements [5].

Due to the complexity, integration and associativity of electric motors in industrial systems, the appropriate maintenance policy for these actuators must be designed to reduce losses and increase product life cycle [6], [7] and [8]. The implementation of a maintenance strategy for monitoring these faults requires a scientific approach involving various tasks, including modelling, signal analysis and processing, decision support and implementation [9] and [10].

Intelligent fault diagnosis refers to the employment of machine learning methods, such as Naive Bayes classifier (NB); Decision Tree classifier (DT); Linear Discriminant Analysis (DA); K-Nearest Neighbors algorithm (KNN); Support Vector Machine (SVM); Ensemble classifier (EN); Preferred Networks (PN); Random Forest classifier (RF); Adaptive Neuro-Fuzzy Inference System (ANFIS) and Neural Network (NN), for machine fault diagnosis [11] and [15], which holds great promise for achieving the above purpose. These types of approaches use machine learning theories to adaptively learn machine diagnostic knowledge from collected data instead of using the experience and knowledge of engineers.

The main objective of this paper is to propose a strategy for monitoring and diagnosis of electrical machines by applying advanced signal processing methods and artificial intelligence approaches, while exploiting vibration signals recovered from sensors placed on the machines. Generally speaking, this study is part of preventive maintenance to ensure the quality of procedures and the availability of machines in real time for the purpose of remote monitoring.

This paper is structured as follows: Section 2. presents the detailed hardware design for the laboratory experimental setup and describes the theoretical background of the origins and effects of the bearing fault and the measurement results using the Envelope Harmonic-to-Noise Ratio (E-HNR) algorithm to detect this fault. Section 3. describes the proposed monitoring architecture of the bearing in the Induction Machine (IM), results and discussion. Finally, the conclusion is given in Sec. 4.

2. Materials and Methods

2.1. Experimental Testbed and Dataset Acquisition

The test bench shown in Fig. 1 was developed at the LASPI (Laboratoire d'analyse des signaux et des processus industriels) laboratory in Universite Jean Monnet-Roanne. It consists of a shaft mounted on two bearings with rolling elements of type "RS-6205". The entire assembly is connected to an electric motor by means of a rigid coupling. The shaft speed is controlled by a variable speed drive. The asynchronous motor used in this experiment has these parameters: 0.25 kW, f=50 Hz and 2780 rpm.

This bench allows the measurement of the following signals: vibrations and currents. It is associated with a NI (National Instruments) acquisition card controlled by LabVIEW with a sampling frequency of f_s =25 600 Hz.
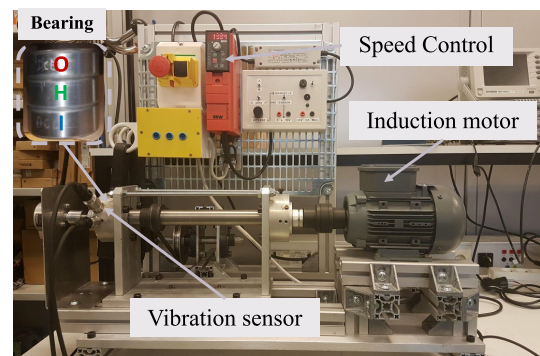

Fig. 1: Experimental test setup for bearing data set.

2.2. Bearing Characteristic Frequencies

The ball bearings serve as an electromechanical interface between the stator and the rotor. In addition, they maintain the axis of the machine to ensure correct rotation of the rotor. Figure 2 shows the components of a bearing.
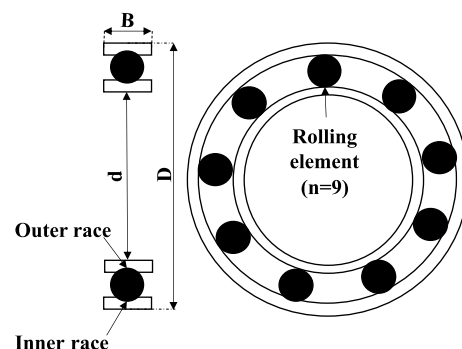

Fig. 2: Elements composing a ball bearing.

The geometric parameters of the bearing are given in Tab. 1 [16]:

Bearing failures have an influence on system vibrations because bearings are connecting and strengthening elements. The vibrations that occur inside a bearing are small in amplitude and resemble ran-

Tab. 1: Geometric parameters of the bearing.

Parameter	Value
Bearing number	6205-2RS
Outside diameter (D)	52 mm
Bore diameter (d)	25 mm
Width (B)	15 mm
Number of balls (N)	9
Contact angle Θ	0
Ball diameter (D_b)	7.94 mm
Pitch diameter (P_d)	39.04 mm

dom noise. In case of degradation, a pulse is produced each time the fault comes into contact. This excites the mechanical resonance frequencies of the structure, which will be modulated by the characteristic frequency of the fault. The fault, therefore, has a characteristic signature which depends on the geometry of the bearing and the location of the spalling (on the inner race, the outer race or a rolling element) [17] and [18]. Ball bearings have a unique frequency corresponding to the dynamic behaviour of each component of the bearing: the characteristic frequency of the outer race ($f_{bo}/BPFO$), the characteristic frequency of the inner race ($f_{bi}/BPFI$), the characteristic frequency of the balls (f_{bsf}/BSF) and the characteristic frequency of the cage (f_{cage}/FTF). The characteristics f_{bo}, f_{bi}, f_{cage}, f_{bsf} depend on the bearing geometry and the rotor frequency f_r.

$$FTF = f_{cage} = \frac{1}{2}f_r\left(1 - \frac{D_b}{D_r}\cos\Theta\right), \qquad (1)$$

$$BPFI = f_{bi} = \frac{1}{2}N \cdot f_r\left(1 + \frac{D_b}{D_r}\cos\Theta\right), \quad (2)$$

$$BPFO = f_{bo} = \frac{1}{2}N \cdot f_r\left(1 - \frac{D_b}{D_r}\cos\Theta\right), \quad (3)$$

$$BSF = f_{bsf} = f_r\frac{D_r}{D_b}\left(1 - \left(\frac{D_b}{D_r}\cos\Theta\right)^2\right). \quad (4)$$

- f_{bo}: Characteristic frequency of the outer race defect,

- f_{bi}: Characteristic frequency of the inner race defect,

- f_r: Cage rotation frequency,

- f_{bsf}: Characteristic frequency of the ball defect,

- N: Number of balls,

- D_b: Ball diameter,

- D_r: Bearing diameter,

- Θ: Contact angle.

2.3. Mathematical Vibration Model for Rolling Element Bearing

In [19], a model produced by a single point defect was proposed. And soon after, the model was extended to describe multiple defect points [18]. Moreover, the mathematical model of the bearing was modified in [20], considering the random sliding of the rolling elements and the cage.

According to the approaches of vibration signal modelling presented in [18], [20] and [22], the generated vibration response $V(t)$ is obtained by the convolution product of the impact pulse series $A(t)$ with the machine impulse response $R(t)$, which is generated by the distance between the acceleration sensor and the defective bearing.

$$V(t) = [A(t) * R(t)] + n(t), \qquad (5)$$

where $R(t)$ describes the impulse response of the machine which can be modelled as a damped sinusoid, oscillating at the resonant frequency F_{res} and damped by a damping ratio ξ.

$$\begin{cases} R(t) = \sin(2\pi F_{res}t) \cdot e^{-vt} \cdot u(t) \\ v = 2\pi F_{res} \cdot \dfrac{\xi}{\sqrt{1 + \xi^2}} \end{cases}, \qquad (6)$$

where v is the damping ratio and $u(t)$ is the Heaviside unit step. The instantaneous shock amplitude $A(t)$ is defined by Eq. (7).

$$\begin{cases} A(t) = m_k(t) \cdot \sum_i a_i \delta(t - iT_{def} - \gamma_i) \\ m_k(t) = 1 + k\cos(2\pi f_r t) \end{cases}, \qquad (7)$$

where f_r is the rotation frequency, $f_{def} = \dfrac{1}{T_{def}}$ is the fault frequency, k represents the modulation rate, i represents the impact indices, a_i is the normally distributed random amplitude ($N(\mu_{ai}, \sigma_{ai}^2)$) and γ_i is the normally distributed random fluctuation ($N(0, \sigma^2\gamma i)$). For a defect in the outer race, the modulation rate k is zero. $n(t)$ represents the white noise in the measurement.

- **Inner race fault:**

  Figure 3 shows the simulated vibration signal with an inner race defect using the parameters presented in Tab. 2. Figure 4 shows a comparison between the envelope spectrum of the simulated signal and the measured signal. We notice a very high correspondence between the two spectra.

- **Outer race fault:**

  Figure 5 shows the simulated vibration signal with an outer race defect using the parameters presented in Tab. 2. Figure 6 shows a comparison

Tab. 2: Geometric parameters of the bearing.

Parameter	μ_{ai} (mv)	σ_{ai} (mv)	$\sigma_{\gamma i}$ (µs)	k	f_r (Hz)	F_{def} (Hz)	F_{res} (Hz)	ξ
Inner-race	7	0.5	0.4	0	33	182	2500	0.3
Outer-race	7	0.5	0.4	0.9	33	119	2500	0.3

between the envelope spectrum of the simulated signal and the measured signal. We notice a very high correspondence between the two spectra.

Bearing manufacturers sometimes do not provide the exact geometry of the bearing elements. However, they often offer calculation tools to find out the characteristic frequencies of a specific bearing depending on its rotational speed.

defects in ball bearings. Figure 7 shows the vibration signals from a normal bearing assumed to be healthy, a bearing with a defect in the inner race and a bearing with a defect in the outer race. It can be seen that the vibration amplitude of the defective bearing is significantly higher than that of the normal bearing, both in terms of peak value and Root Mean Square (RMS) value.
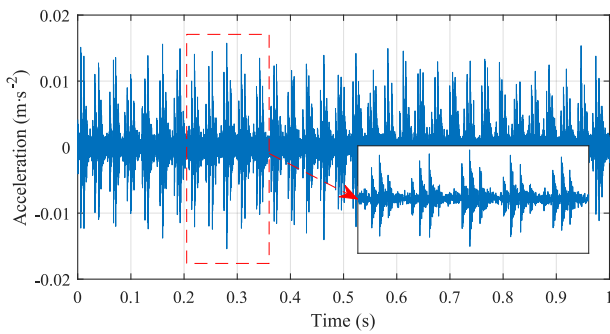

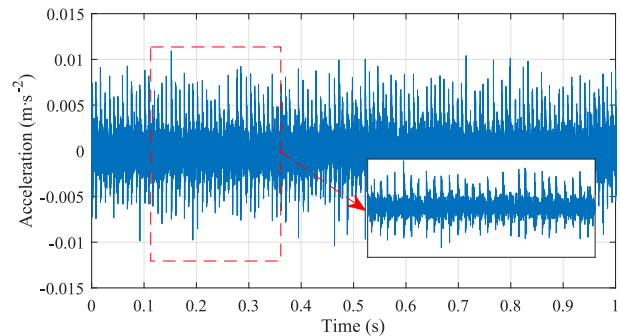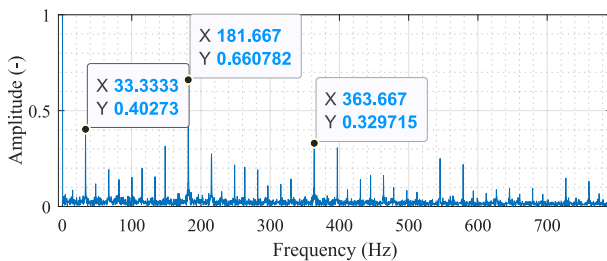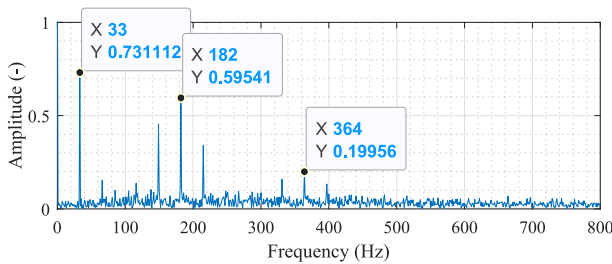**Fig. 3:** Simulated vibration signal with inner race fault.

Fig. 5: Simulated vibration signal with outer race fault.
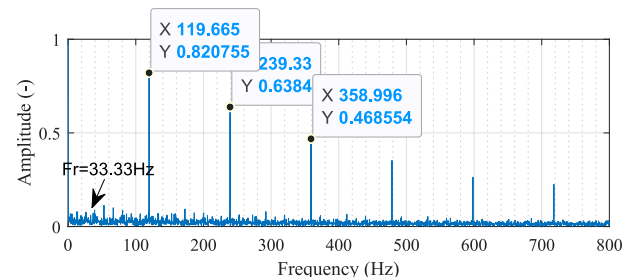

(a) Measured results.

(a) Measured results.

(b) Simulation results.

Fig. 4: Comparison of the envelope spectra of a faulty ball bearing (type SKF RS6205) with an inner race fault with 33.33 Hz rotation frequency.
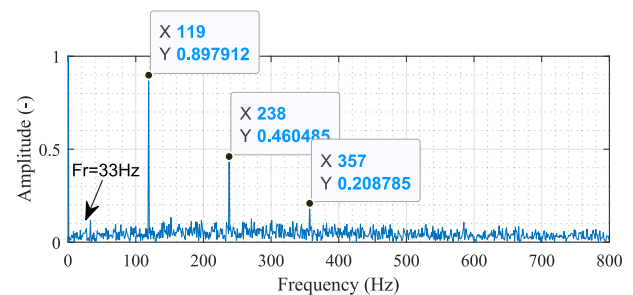

(b) Simulation results.

Fig. 6: Comparison of the envelope spectra of a faulty ball bearing (type SKF RS6205) with an outer race fault with 33.33 Hz rotation frequency.

2.4.   Experimental Results Analysis

Considering the experimental measurements carried out using the "LASPI" laboratory test bench to study

In the frequency domain, the presence of peaks in the vibration spectrum can be used to identify both the type of defect and its location. For the detection and diagnosis of bearing faults, the characteristic fre-

quencies associated with specific faults must be known, for a mechanical rotation frequency of $f_r = 33.33$ Hz, the outer race, inner race, cage and ball frequencies are respectively $f_{bo} = 119$ Hz, $f_{bi} = 181$ Hz, $f_c = 13$ Hz and $f_{bsf} = 78$ Hz.
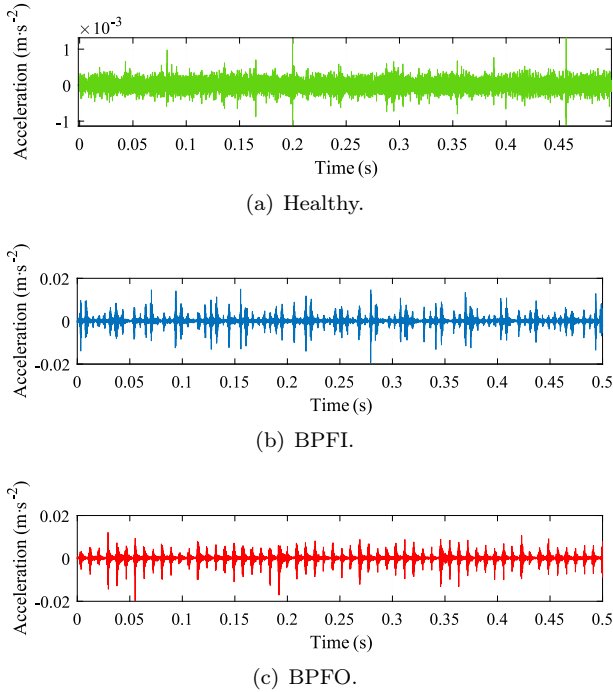

(a) Healthy.

(b) BPFI.

(c) BPFO.

Fig. 7: Comparison of the envelope spectra of a faulty ball bearing (type SKF RS6205) with an outer race fault with 33.33 Hz rotation frequency.

The progression of bearing defect degradation will lead not only to the growth of vibration amplitude at bearing frequencies, but also to the generation of vibrations at harmonics of these frequencies. Figure 8 shows the vibration envelope spectrum of a normal bearing assumed to be healthy, a bearing with a defect in the inner race and a bearing with a defect in the outer race. The initial dominant peak in the spectrum can be easily identified by the difference between the healthy and defective spectrum.
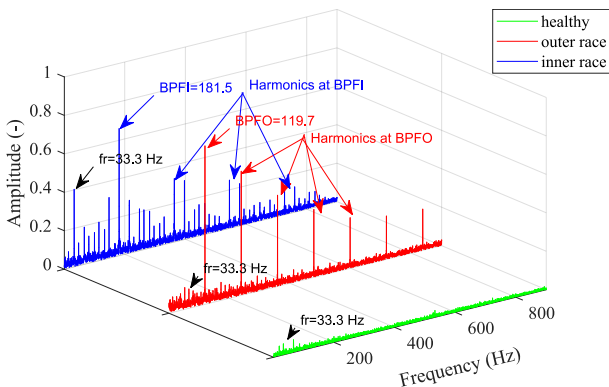

Fig. 8: Envelope spectrum of healthy signal, signal with inner race fault and signal with outer race fault.

2.5. Envelope Harmonic-to-Noise Ratio (E-HNR)

The E-HNR is suitable for characterising the periodicity of bioacoustics because the signal is mainly harmonic and noisy. It has been widely used in the field of mechanical fault diagnosis [23], automatic speech recognition and human phonetics as a diagnostic tool for the quantification of voice changes [24]. Since fault-induced periodic pulses are usually modulated at resonant frequencies, E-HNR has been proposed to eliminate the modulation effect [25] and [26].

The E-HNR algorithm can be run as follows:

- Extract the envelope signal $E[x(t)]$ by the Hilbert Transform from the measured signal $x(t)$ and remove the continuous component,

$$x^{`}(t) = H\{x(t)\} = \frac{1}{\pi} \int_{-\infty}^{+\infty} \frac{x(\tau)}{t - \tau} \int d\tau, \quad (8)$$

$$E[x(t)] = \sqrt{x^2(t) + x^{`2}(t)}, \quad (9)$$

$$E[x(t)] = E[x(t)] - \text{mean}\{E[x(t)]\}. \quad (10)$$

- Calculation of the autocorrelation of $E[x(t)]$:

$$r_{E[x(t)]}(\tau) = \int E[x(t)]E[x(t + \tau)]dt. \quad (11)$$

Then, the E-HNR can be represented by:

$$EHNR = \frac{r_{E[x(t)]}(\tau_{\max})}{r_{E[x(t)]}(0) - r_{E[x(t)]}(\tau_{\max})^{`}}, \quad (12)$$

where τ is the delay time, $\tau_{\max}$ is the delay time of the maximum of the autocorrelation function, $x'(t)$ is the Hilbert transform of $x(t)$, $E[x(t)]$ is the amplitude of the Hilbert transform and $rE[x(t)](\tau)$ is the autocorrelation function of $E[x(t)]$.

Figure 9 and Fig. 10 show the results of applying the HNR-based method to the vibration signals of the tested bearings.

Figure 9 shows the result of the HNR-based method in the case of outer race bearing fault. Figure 9(b) shows the filtered signal with a band-pass filter with frequency center $f_c = 6000$ Hz and bandwidth $B_w = 800$ Hz, at the decomposition level $(k = 4)$. Figure 9(c) shows its envelope spectrum. Spectral lines at the frequencies (BPFO) appear clearly on the spectrum and represent the outer race bearing fault of frequency $f_{be} = 119$ Hz and its high order harmonics.

Figure 10 shows the result of the HNR-based method in the case of inner race bearing fault. Figure 10(b) shows the filtered signal with a bandpass filter with
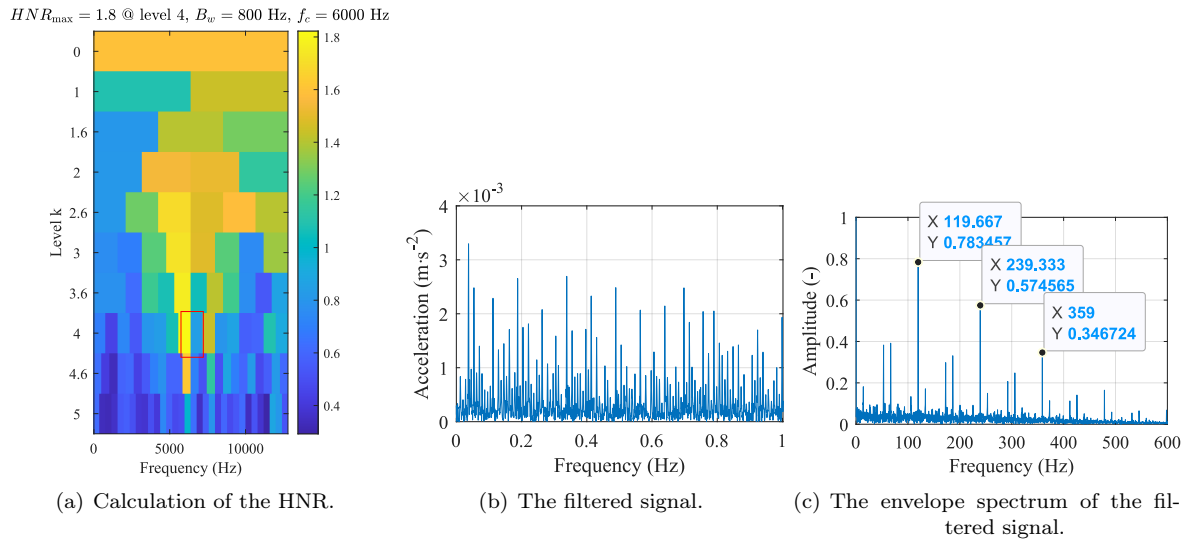
(a) Calculation of the HNR.

(b) The filtered signal.

(c) The envelope spectrum of the filtered signal.

Fig. 9: Results of the application of the HNR-based method (BPFO fault case).

(a) Calculation of the HNR.

(b) The filtered signal.

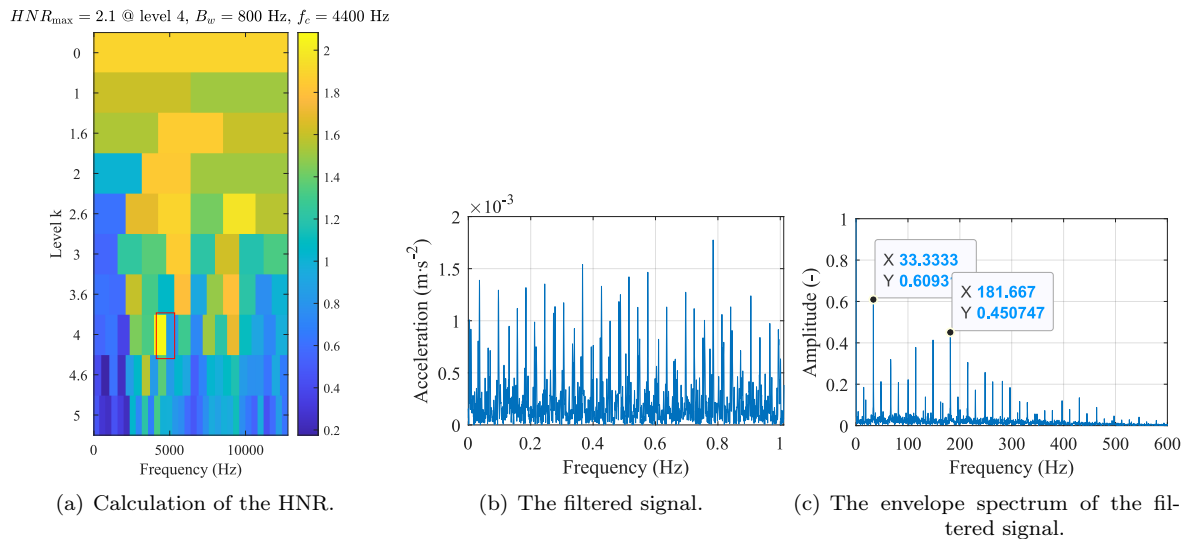(c) The envelope spectrum of the filtered signal.

Fig. 10: Results of the application of the HNR-based method (BPFI fault case).

a center frequency $f_c = 4400$ Hz and a bandwidth $B_w = 800$ Hz, at the decomposition level ($k = 4$). Figure 10(c) shows its envelope spectrum. We observe spectral lines at frequencies (BPFI) appearing clearly on the spectrum and represent the inner race bearing fault of frequency $f_{bi} = 181$ Hz and its high order harmonics.

3.   Proposed Architecture

The objective of this work is to propose a strategy for the monitoring and diagnosis of IM by applying advanced signal processing methods and artificial intelligence approaches, while exploiting the vibration signals recovered from the sensors placed on the machine.

3.1.   Description of the Proposed Algorithm

The objective of this study consists in designing a robust model for the detection of rolling defects by combining several classifiers. The developed architecture shown in Fig. 11 aims to reduce the classification problem from three classes to two classes. It is based, first, on the extraction of fault indicators from the vibration envelope signals by applying the E-HNR algorithm. Normalisation is then applied to the extracted indicators to create a well-processed data set. It is possible to select the most informative indicators from the set of indicators extracted from the vibration signal. Once the indicator selecting and merging tasks are completed, two classes of fault detection are considered. In the first scenario (1st class), the selected and merged

indicators are sent directly to the ten classifiers to determine whether the machine is in a normal or faulty state. In the second scenario (2nd class), if the decision made by the 1st class is that the motor is defective, a second classification will be made to detect the type of bearing condition (outer race BPFO defect or inner race BPFI defect).
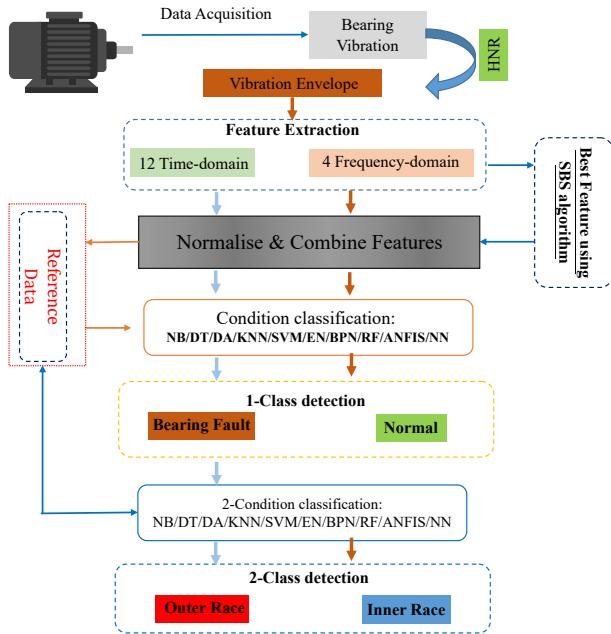

Fig. 11: Proposed intelligent architecture for bearing fault detection.

3.2. Description of the Bearing Dataset

The bearing data set was acquired from the experimental system under three different operating conditions: (A) normal condition, (B) with outer race defect and (C) with inner race defect. Each bearing was tested under four different speeds: 1060, 1480, 2000, and 2500 rpm, respectively. The data sets A, B and C are described in Tab. 3.

Data sets B and C contain 240 data samples with the same fault size at four different speeds. Data sets A, B and C are separated into two data subsets: 120 samples for training and 120 samples for testing, with a total of 360 signals for training and 360 signals for testing. This is a simple three-class classification problem corresponding to the three different categories of faults. In order to increase reliability, the combination of several classifiers has been increasingly studied to overcome the limitations of the individual classifier and to achieve higher classification accuracy. It is suggested that these classifiers, which are different in their input feature set or classification algorithm, generally have complementary classification behaviour.

3.3. Extraction of Indicators

In recent years, the E-HNR has been widely studied for condition monitoring and fault diagnosis [23], [25] and [26]. However, it is still difficult for us to select an appropriate characteristic due to the different mechanical failures, as the different faults have their own time and frequency domain effects.

To monitor the health of the machines, 16 common statistical features are extracted from the time and frequency domains of the original vibration signals. Twenty statistical features in the time domain include Peak (F1), Peak-peak (F2), Mean (F3), Standard deviation (F4), Root mean square (F5), Root Amplitude (F6), Skewness (F7), Kurtosis (F8), Crest factor (F9), Clearance factor (F10), Impulse factor (F11), Shape factor (F12). Successively, four common statistical features of the frequency domain, including Mean frequency (F13), Standard deviation frequency (F14), frequency center (F15), Root mean square frequency (F16), as shown in Tab. 4, are also extracted from the FFT spectra of the original E-HNRs of the vibration and current signals.
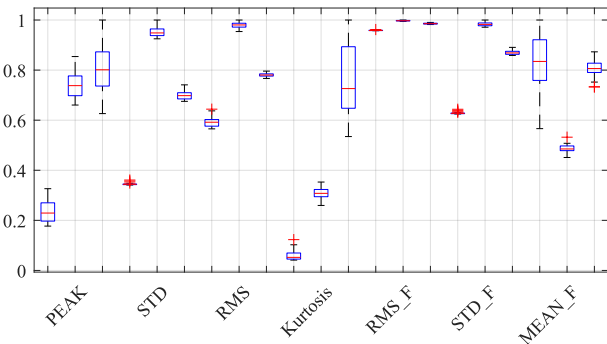

Fig. 12: Box-Whisker plot of the indicators extracted from the envelope signal obtained by HNR, on the left healthy state, middle with BPFO fault and on the right with BPFI fault.

Figure 12 shows a Box-Whisker plot of the indicators extracted from the vibration envelope signal obtained by HNR, normalised according to the min/max normalisation. For each indicator, we have on the left the healthy state, in the middle the BPFO fault and on the right the BPFI fault. Each box highlights five of the parameters of a statistical series: minimum, first quartile, median (red line), third quartile and maximum. From the figure, it is easy to differentiate between the three states (healthy, BPFO and BPFI) for several indicators.

Tab. 3: Introduction to datasets.

Database	Number of training signals	Number of test signals	Rotational speed (rpm)	Operating state	Classification label
A	30	30	1060	Healthy state	1
	30	30	1480	Healthy state	1
	30	30	2000	Healthy state	1
	30	30	2500	Healthy state	1
B	30	30	1060	BPFO fault	2
	30	30	1480	BPFO fault	2
	30	30	2000	BPFO fault	2
	30	30	2500	BPFO fault	2
C	30	30	1060	BPFI fault	3
	30	30	1480	BPFI fault	3
	30	30	2000	BPFI fault	3
	30	30	2500	BPFI fault	3

Tab. 4: Time domain and frequency domain statistical parameters.

Time domain statistical parameters

Peak	$F_1 = \max |x(n)|$	Peak-peak	$F_2 = \max(x(n)) - \min(x(n))$
Mean	$F_3 = \frac{\sum_{n=1}^{N} x(n)}{N}$	Standard deviation	$F_4 = \sqrt{\frac{\sum_{n=1}^{N}(x(n)-F_3)^2}{N-1}}$
Root mean square	$F_5 = \sqrt{\frac{\sum_{n=1}^{N}(x(n))^2}{N}}$	Root Amplitude	$F_6 = \left(\frac{\sum_{n=1}^{N}\sqrt{|x(n)|}}{N}\right)^2$
Skewness	$F_7 = \frac{\sum_{n=1}^{N}(x(n)-F_3)^3}{(N-1)F_4^3}$	Kurtosis	$F_8 = \frac{\sum_{n=1}^{N}(x(n)-F_3)^4}{(N-1)F_5^4}$
Crest factor	$F_9 = \frac{F_1}{F_5}$	Clearance factor	$F_{10} = \frac{F_1}{F_6}$
Impulse factor	$F_{11} = \frac{F_2}{\left(\sum_{n=1}^{N}|x(n)|\right)/N}$	Shape factor	$F_{12} = \frac{F_6}{\left(\sum_{n=1}^{N}|x(n)|\right)/N}$

where $x(n)$ is a signal series for $n = 1, 2, \ldots, N$, N is the number of data points.

Frequency domain statistical parameters

Mean frequency	$F_{13} = \frac{\sum_{k=1}^{K} s(k)}{K}$	Standard deviation frequency	$F_{14} = \sqrt{\frac{\sum_{k=1}^{K} f_k^2 s(k)}{\sum_{k=1}^{K} s(k)}}$
Frequency center	$F_{15} = \frac{\sum_{k=1}^{K} f_k s(k)}{\sum_{k=1}^{K} s(k)}$	Root mean square frequency	$F_{16} = \sqrt{\frac{\sum_{k=1}^{K}(f_k - F_{15})^2 s(k)}{\sum_{k=1}^{K} s(k)}}$

where $s(k)$ is a spectrum for $k = 1, 2, \ldots, K$, K is the number of spectrum lines; fk is the frequency value of the kth spectrum line.

3.4. Selection of Informative Indicators

the most informative indicators from a set of indicators extracted from the vibration signal. For this purpose, we have chosen the SBS (Sequential Backward Selection) method [27] and [29]. This method was applied to a vector composed of indicators extracted by the SBS method to extract the six best features. We have applied a supervised version of SBS.

Figure 13 shows that the first three best indicators selected make it possible to differentiate between the "healthy" state and the "defective" states BPFO and BPFI. The evolution of the "defective" state follows a linear trajectory.

Fig. 13: Projection of the normalised indicators (Kurtosis, STD and RMS frequency) into the subspace of dimension 3. (Healthy bearing, with BPFO fault and with BPFI fault).

3.5. Supervised Machine Learning

Supervised machine learning consists of removing a certain portion of the training data and using it as test data. The model is first trained on the training data set and then asked to predict the results of the test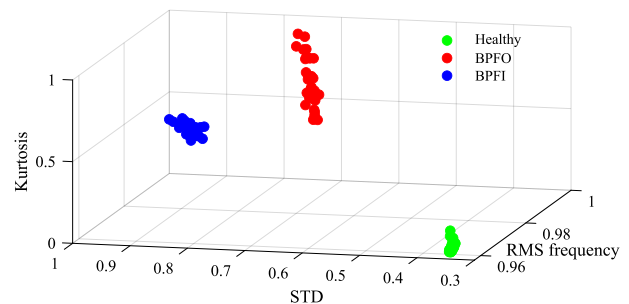 data set. This is the simplest form of validation technique and is useful if a large amount of data is available or if the implementation needs to be implemented quickly and easily. The classification algorithm learns to associate the input features with the corresponding label, which consists of a class label representing the type of fault. The result is a classification model that can be used to predict the type of fault for a given input signal [26] and [30].

In our work, ten classifiers mentioned above have been tested and applied: NB, DT, DA, KNN, SVM, EN, PN, RF, ANFIS, and NN. All classification algorithms were tested using a random sampling approach. The dataset was divided into 50 % for training and 50 % for testing.

3.6. Results and Discussion

The method we are interested in for fault detection is the classification. In particular, classification is evaluated by verifying a priori whether the classes assigned to the observations are the correct ones. Regarding machine learning, a classification approach learns and predicts the so-called positive or negative labels. The behaviours that we consider as positive in our work are healthy behaviours and negative in case of defects. The results obtained by the detection are then classified in a confusion matrix composed of the following main parameters [15] and [31]:

- True Negative (TN): is an outcome where the model correctly predicts the negative class.

- True Positive (TP): is an outcome where the model correctly predicts the positive class.

- False Positive (FP): is an outcome where the model incorrectly predicts the positive class.

- False Negative (FN): is an outcome where the model incorrectly predicts the negative class.

Different statistics can be obtained from these main measures. Among those used in our field, we find Accuracy, Sensitivity and Specificity.

$$\text{Accuracy} = \frac{TP + TN}{TP + TN + FP + FN}, \qquad (13)$$

$$\text{Specificity} = \frac{TP}{TP + FP}, \qquad (14)$$

$$\text{Sensitivity} = \frac{TP}{TP + FN}. \qquad (15)$$

In the first scenario (1st class), as this classification problem is relatively easy, the ten individual classifiers obtain correct test results ranging from 71.43 % up to 100 %. As shown in Fig. 14 (1st class), five classifiers (DA, KNN, SVM, BPN, ANFIS and NN) have 100 % accuracy in the test.

In the second scenario (2nd class), one classifier (NN) obtained a 100 % correct test result, as shown in Fig. 14 (2nd class).

These experimental results suggest that reducing the degree of the classification problem improved the accuracy of the classifiers. Therefore, in order
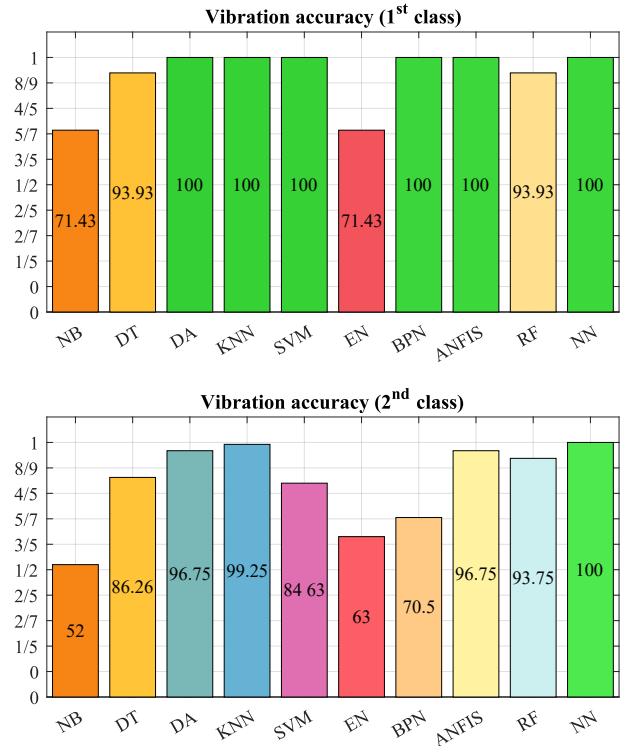

Fig. 14: Results of the proposed intelligent architecture for bearing fault detection (%).

to achieve maximum accuracy that reaches 100 %, we only need to combine two classifiers that have an accuracy of 100 % in each class.
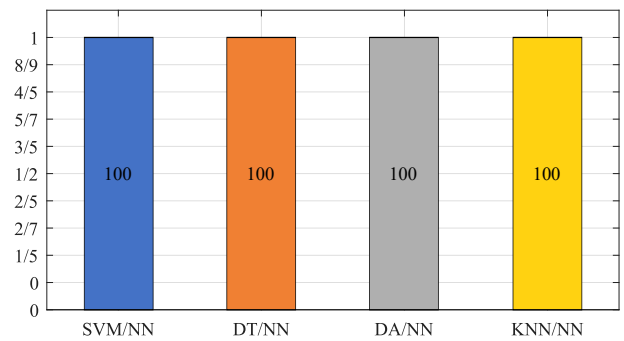

Fig. 15: Test of the proposed intelligent architecture for bearing fault detection (%).

To test the performance of the proposed architecture based on the combination of two classifiers, we choose the SVM, DT, DA, or KNN classification algorithm for the first scenario (1st class), and the NN algorithm for the second scenario (2nd class). According to Fig. 15, we can see that our architecture was able to correctly classify all test signals, which means that we successfully detected all conditioning states of our machine.

3.7. Comparison with other Feature Selection and Fault Diagnosis Methods

In order to compare the performance of feature selection and fault diagnosis with other approaches, we present 4 additional strategies, which have already been studied by other researchers. In Method 1, authors [32] used Preselect features using ReliefF filter + Reselect features and optimized SVM parameters synchronously using Binary Particle Swarm Optimization (BPSO) + Diagnose fault types using the optimal feature subsets and the trained SVM model. In Method 2, authors [33] present a novel pattern classification approach for bearings diagnostics, which combines the higher-order spectra analysis features and SVM classifier. In Method 3, a novel fault diagnosis technique based on Improved Multiscale Dispersion Entropy (IMDE) and Max-Relevance Min-Redundancy (mRMR) is proposed [34]. Firstly, the IMDE method is developed to capture multi-scale fault features from the collected original vibration signal. Then, the mRMR algorithm is utilized to automatically select the sensitive features from the candidate multi-scale features without any prior knowledge. Finally, the sensitive feature vector set after normalisation treatment is inputted into the Extreme Learning Machine (ELM) classifier to train the intelligent diagnosis model and provide fault diagnosis results. In Method 4, ICGOA-KELM (Improved Circle Chaotic map with Grasshopper Optimization Algorithm- Kernel Extreme Learning Machine) is introduced as a fault classification method and is combined with Variational Modal Decomposition (VMD), Multi-scale Permutation Entropy (MPE) and Kernel Principal Component Analysis (KPCA) as a new hybrid intelligent fault diagnosis method for rolling bearings [35].

Tab. 5: Comparison of our results with previous research.

Fault diagnosis architecture	Number of optimal features	Average testing accuracy
Proposed method	6	100.00 %
Method 1	4	98.57 %
Method 2	5	96.98 %
Method 3	9	100.00 %
Method 4	3	100.00 %

4. Conclusion

The objective of this study was to propose a strategy for monitoring and diagnosing the bearings of electrical machines by using advanced signal processing methods and artificial intelligence approaches, while exploiting the vibration signals recovered from sensors placed on the machine. In addition, the proposed algorithms must be fast, simple to implement, with relatively low memory consumption. In other words, they must respect the constraints of an online condition monitoring system in order to present an efficient and economical solution that deserves its place in Industry 4.0.

After validating the experimental results with the results obtained via our bearing vibration simulation model, we have exploited the indicator selection method to take advantage of the best diagnostic techniques. In this work, we have proposed an intelligent architecture for bearing fault detection by combining several classifiers to detect the bearing condition (Outer race defect BPFO, Inner race defect BPFI or Healthy state). The experimental results verify the relevance of the proposed approach.

Acknowledgment

Author Contributions

The theoretical studies and numerical results presented in this article were carried out by I. O. in the Energy Optimization, Diagnosis and Control (EODIC) research team of the ENSAM-Rabat research center, under the supervision of Ms. S. EL H. K. D. has provided critical comments, contributed to the development of the acquisition software and the writing of the final version of the manuscript.

References

[1] ADEME. *Les Chiffres Cles 2016: Climat, Air et Energie.* 1st ed. Angers: ADEME Editions, 2016. ISBN 979-1-0297-0310-2.

[2] SAAD, N., M. IRFAN and R. IBRAHIM. *Condition Monitoring and Faults Diagnosis of Induction Motors: Electrical Signature Analysis.* 1st ed. Boca Raton: CRC Press, 2018. ISBN 978-0-8153-8995-8.

[3] KRAUSE, P. C., O. WASYNCZUK and S. D. SUDHOFF. *Analysis of Electric Ma-*

chinery and Drive Systems. 2nd ed. Hoboken: Wiley-IEEE Press, 2013. ISBN 978-0-471-14326-0.

[4] YUNG, C. and A. H. BONNETT. Repair or replace? *IEEE Industry Applications Magazine*. 2004, vol. 10, iss. 5, pp. 48–58. ISSN 1558-0598. DOI: 10.1109/MIA.2004.1330770.

[5] TOLIYAT, H. A., S. NANDI, S. CHOI and H. MESHGIN-KELK. *Electric Machines: Modeling, Condition Monitoring, and Fault Diagnosis*. 1st ed. Boca Raton: CRC press, 2013. ISBN 978-1-138-07397-5.

[6] YANG, B.-S. and A. WIDODO. *Introduction to Intelligent Machine Fault Diagnosis and Prognosis*. 1st ed. Hauppauge: Nova Science Publishers, Inc., 2011. ISBN 978-1-60692-263-7.

[7] TOMA, R. N., A. E. PROSVIRIN and J.-M. KIM. Bearing Fault Diagnosis of Induction Motors Using a Genetic Algorithm and Machine Learning Classifiers. *Sensors*. 2020, vol. 20, iss. 7, pp. 1–19. ISSN 1424-8220. DOI: 10.3390/s20071884.

[8] OUACHTOUK, I., S. EL HANI, S. GUEDIRA, K. DAHI and L. SADIKI. Advanced Model of Squirrel Cage Induction Machine for Broken Rotor Bars Fault Using Multi Indicators. *Advances in Electrical and Electronic Engineering*. 2016, vol. 14, iss. 5, pp. 512–521. ISSN 1804-3119. DOI: 10.15598/aeee.v14i5.1705.

[9] KANNAN, R., S. S. MANOHAR and M. S. KUMARAN. IoT-Based Condition Monitoring and Fault Detection for Induction Motor. In: *Proceedings of 2nd International Conference on Communication, Computing and Networking*. Singapore: Springer, 2019, pp. 205–215. ISBN 978-981-13-1217-5. DOI: 10.1007/978-981-13-1217-5_21.

[10] MERIZALDE, Y., L. HERNANDEZ-CALLEJO and O. DUQUE-PEREZ. State of the Art and Trends in the Monitoring, Detection and Diagnosis of Failures in Electric Induction Motors. *Energies*. 2017, vol. 10, iss. 7, pp. 1–34. ISSN 1996-1073. DOI: 10.3390/en10071056.

[11] KATERIS, D., D. MOSHOU, X.-E. PANTAZI, I. GRAVALOS, N. SAWALHI and S. LOUTRIDIS. A machine learning approach for the condition monitoring of rotating machinery. *Journal of Mechanical Science and Technology*. 2014, vol. 28, iss. 1, pp. 61–71. ISSN 1738-494X. DOI: 10.1007/s12206-013-1102-y.

[12] JIANG, F., Y. JIANG, H. ZHI, Y. DONG, H. LI, S. MA, Y. WANG, Q. DONG, H. SHEN and Y. WANG. Artificial intelligence in healthcare: past, present and future. *Stroke and Vascular Neurology*. 2017, vol. 2, iss. 4, pp. 230–243. ISSN 2059-8688. DOI: 10.1136/svn-2017-000101.

[13] ZARE, S. *Fault Detection and Diagnosis of Electric Drives Using Intelligent Machine Learning Approaches*. Windsor, 2018. Dissertation. University of Windsor. Supervisor Dr. Mehrdad Saif.

[14] FERGUSON, A. L. Machine learning and data science in soft materials engineering. *Journal of Physics: Condensed Matter*. 2017, vol. 30, iss. 4, pp. 1–50. ISSN 1361-648X. DOI: 10.1088/1361-648X/aa98bd.

[15] RAFIQUE, D. and L. VELASCO. Machine Learning for Network Automation: Overview, Architecture, and Applications [Invited Tutorial]. *Journal of Optical Communications and Networking*. 2018, vol. 10, iss. 10, pp. 126–134. ISSN 1943-0639. DOI: 10.1364/JOCN.10.00D126.

[16] 6205 - Deep groove ball bearings. In: *SKF* [online]. 2021. Available at: https://www.skf.com/group/products/rolling-bearings/ball-bearings/deep-groove-ball-bearings/productid-6205.

[17] CORNE, B., B. VERVISCH, C. DEBRUYNE, J. KNOCKAERT and J. DESMET. Comparing MCSA with vibration analysis in order to detect bearing faults – A case study. In: *2015 IEEE International Electric Machines & Drives Conference (IEMDC)*. Coeur d'Alene: IEEE, 2015, pp. 1366–1372. ISBN 978-1-4799-7941-7. DOI: 10.1109/IEMDC.2015.7409240.

[18] MCFADDEN, P. D. and J. D. SMITH. The vibration produced by multiple point defects in a rolling element bearing. *Journal of Sound and Vibration*. 1985, vol. 98, iss. 2, pp. 263–273. ISSN 0022-460X. DOI: 10.1016/0022-460X(85)90390-6.

[19] MCFADDEN, P. D. and J. D. SMITH. Model for the vibration produced by a single point defect in a rolling element bearing. *Journal of Sound and Vibration*. 1984, vol. 96, iss. 1, pp. 69–82. ISSN 0022-460X. DOI: 10.1016/0022-460X(84)90595-9.

[20] ANTONI, J. and R. B. RANDALL. A Stochastic Model for Simulation and Diagnostics of Rolling Element Bearings With Localized Faults. *Journal of Vibration and Acoustics*. 2003, vol. 125, iss. 3, pp. 282–289. ISSN 1528-8927. DOI: 10.1115/1.1569940.

[21] ZHAO, M., J. LIN, X. XU and X. LI. Multi-Fault Detection of Rolling Element Bearings under Harsh Working Condition Using IMF-Based

Adaptive Envelope Order Analysis. *Sensors*. 2014, vol. 14, iss. 11, pp. 20320–20346. ISSN 1424-8220. DOI: 10.3390/s141120320.

[22] HAD, A. and K. SABRI. A two-stage blind deconvolution strategy for bearing fault vibration signals. *Mechanical Systems and Signal Processing*. 2019, vol. 134, iss. 1, pp. 1–20. ISSN 0888-3270. DOI: 10.1016/j.ymssp.2019.106307.

[23] MIAO, Y., M. ZHAO, J. LIN, K. LIANG and G. LIU. Harmonics-to-noise ratio guided deconvolution and its application for bearing fault detection. In: *2017 Prognostics and System Health Management Conference (PHM-Harbin)*. Harbin: IEEE, 2017, pp. 1–8. ISBN 978-1-5386-0370-3. DOI: 10.1109/PHM.2017.8079259.

[24] BOERSMA, P. Accurate short-term analysis of the fundamental frequency and the harmonics-to-noise ratio of a sampled sound. In: *Proceedings of the institute of phonetic sciences*. Amsterdam: Citeseer, 1993, pp. 97–110.

[25] SUN, P., Y. LIAO and J. LIN. The Shock Pulse Index and Its Application in the Fault Diagnosis of Rolling Element Bearings. *Sensors*. 2017, vol. 17, iss. 3, pp. 1–23. ISSN 1424-8220. DOI: 10.3390/s17030535.

[26] XU, X., M. ZHAO, J. LIN and Y. LEI. Envelope harmonic-to-noise ratio for periodic impulses detection and its application to bearing diagnosis. *Measurement*. 2016, vol. 91, iss. 1, pp. 385–397. ISSN 0263-2241. DOI: 10.1016/j.measurement.2016.05.073.

[27] CHOUAIB, H. *Selection de caracteristiques: méthodes et applications*. Paris, 2011. Dissertation. Universite Paris Descartes. Supervisor Dr. Florence Cloppet.

[28] DOAK, J. *An evaluation of feature selection methods and their application to computer security*. Oakland, 1992. Dissertation. University of California. Supervisor Dr. Biswanath Mukherjee.

[29] SOUALHI, A. *Du diagnostic au pronostic de pannes des entrainements electriques*. Lyon, 2013. Dissertation. Universite Claude Bernard-Lyon 1. Supervisor prof. Guy Clerc.

[30] CAESARENDRA, W., B. K. PAPPACHAN, T. WIJAYA, D. LEE, T. TJAHJOWIDODO, D. THEN and O. M. MANYAR. An AWS Machine Learning-Based Indirect Monitoring Method for Deburring in Aerospace Industries Towards Industry 4.0. *Applied Sciences*. 2018, vol. 8, iss. 11, pp. 1–19. ISSN 2076-3417. DOI: 10.3390/app8112165.

[31] OUACHTOUK, I., S. EL HANI, S. GUEDIRA and K. DAHI. Detection and classification of broken rotor bars faults in induction machine using K-means classifier. In: *2016 International Conference on Electrical and Information Technologies (ICEIT)*. Tangiers: IEEE, 2016, pp. 180–185. ISBN 978-1-4673-8469-8. DOI: 10.1109/EITech.2016.7519586.

[32] ZHANG, X., Q. ZHANG, M. CHEN, Y. SUN, X. QIN and H. LI. A two-stage feature selection and intelligent fault diagnosis method for rotating machinery using hybrid filter and wrapper method. *Neurocomputing*. 2018, vol. 275, iss. 1, pp. 2426–2439. ISSN 0925-2312. DOI: 10.1016/j.neucom.2017.11.016.

[33] SAIDI, L., J. B. ALI and F. FNAIECH. Application of higher order spectral features and support vector machines for bearing faults classification. *ISA Transactions*. 2015, vol. 54, iss. 1, pp. 193–206. ISSN 0019-0578. DOI: 10.1016/j.isatra.2014.08.007.

[34] YAN, X. and M. JIA. Intelligent fault diagnosis of rotating machinery using improved multiscale dispersion entropy and mRMR feature selection. *Knowledge-Based Systems*. 2019, vol. 163, iss. 1, pp. 450–471. ISSN 0950-7051. DOI: 10.1016/j.knosys.2018.09.004.

[35] CHEN, P., X. ZHAO and Q. ZHU. A novel classification method based on ICGOA-KELM for fault diagnosis of rolling bearing. *Applied Intelligence*. 2020, vol. 50, iss. 9, pp. 2833–2847. ISSN 0924-669X. DOI: 10.1007/s10489-020-01684-6.

About Authors

Ilias OUACHTOUK was born in Foum Zguid-Tata, Morocco, in 1991. He received his M.Sc. degree in electrical engineering from the Mohammed V University in Rabat, Morocco, in 2014. Where he is currently working toward the Ph.D. degree, in the department of electrical engineering. Since 2015, his research interests include modeling and diagnosis of electrical drives, in particular, synchronous and asynchronous motors.

Soumia EL HANI has been Professor at the ENSET (Ecole Normale Superieure de l'Enseignement Technqique, Rabat, Morroco) since October 1992. She is a Research Engineer at the Mohammed V University in Rabat, Morocco, in charge of the research team electromechanical, control and diagnosis, IEEE member, member of the research laboratory in electrical

engineering at ENSET, Rabat. Author of several publications in the field of electrical engineering, including robust control systems, diagnosis and control systems of wind electric conversion. She has been general co Chair of several editions of "the International Conference on Electrical and Information Technologies" from 2016 to 2020.

Khalid DAHI born in 1988, is currently an Associate professor in signal processing and instrumentation at Ecole Centrale Casablanca, Morocco. He received his Ph.D. degree from the Mohammed V University, Morocco, in 2017. His research interests are related to electrical machines and drives, machine condition monitoring, diagnosis, and prognosis.